

SYNTHESIS, CHARACTERISATION AND ANTIBACTERIAL ACTIVITY OF SILVER NANOPARTICLES SYNTHESISED FROM STEM BARK EXTRACTS OF THE AFRICAN CORAL TREE, *ERYTHRINA CAFFRA*

S. SHAIK*, N. ZWANE, N. SINGH

School of Life Sciences, University of KwaZulu-Natal, Westville Campus, Private Bag X54001, Durban 4000, South Africa

Aqueous stem bark extracts of *Erythrina caffra* were used to biosynthesize and characterise silver nanoparticles in addition to investigating the effects of synthesis temperature and incubation time on their yield, size and shape. Furthermore, the antibacterial activity of the synthesized nanoparticles was tested against different bacteria. Synthesis at both ambient temperature and 80 °C resulted in significant nanoparticle yield decreases from 587±2.5 and 578±2 mg after 6 h to 567±2.7 and 520±7 mg after 24 h, respectively, while incubation for 6 and 24 h at ambient temperature yielded more nanoparticles (587±2.5 and 567±2.7 mg, respectively) compared to the same incubation times at 80 °C (578±2 and 520±7 mg, respectively). Transmission electron microscopy revealed spherically shaped nanoparticles which was not affected by synthesis temperature nor incubation time. At both tested temperatures, 67-97% of the nanoparticles were <16 nm in diameter and an increase in incubation time increased nanoparticle size; the largest mean sizes were produced after 24 h (14.6 and 12.6 nm for ambient temperature and 80 °C, respectively). Fourier Transform Infra-Red spectroscopy showed a range of identical functional groups at all incubation times at ambient temperature while at 80 °C, there was some commonality amongst incubation times. Only nanoparticles synthesized at ambient temperature exhibited antibacterial activity against methicillin-resistant *Staphylococcus aureus*, *S. aureus* and *Escherichia coli* displaying zones of inhibition ranging from 14.0±1.0-16.0±0.0, 13.7±1.2-15.0±1.0 and 13.3±0.6-15.3±1.2 mm, respectively, however, there were no significant differences in this activity across the tested incubation times.

(Received July 30, 2019; Accepted November 29, 2019)

Keywords: Green synthesis, Incubation, Nanotechnology, Antimicrobial activity

1. Introduction

Metal nanoparticles have attracted considerable global attention in chemistry, physics and medicine primarily due to their application value resulting from their minute sizes (1 to 100 nm) [1]. Their small sizes afford large surface area to volume ratios which contribute to higher reactivity and unique physical and chemical properties [2]. Metal nanoparticles are commonly produced using physical and chemical methods but, not only are these expensive, hazardous by-products are released into the environment [3]. Green synthesis is an eco-friendly alternative in which reducing metabolites produced naturally by biological organisms such as plants, fungi, bacteria and algae can be used to obtain metal nanoparticles in a readily scalable process [2]. In plants, the reducing metabolites (terpenoids, flavonoids, polyphenols, sugars, alkaloids, phenolic acids and proteins) in the extracts of different parts reduce the metals in metal salts e.g. silver nitrate (AgNO₃) from a charged state (Ag⁺) into its atomic form (Ag). This is followed by nucleation of the atoms and subsequent growth when amalgamation of smaller nanoparticles form thermodynamically stable ones [4]. Final steps include agglomeration of the nanoparticles into various shapes for example spheres, rods, triangles and hexagons and stabilisation facilitated by

* Corresponding author: shaiksh@ukzn.ac.za

the coating of functional groups e.g. carboxylic acids, phenols and amines [5] derived from the plant extract.

Numerous medicinal plants have been used to synthesise metal nanoparticles and these have been extensively reviewed [2, 3, 6-9]. The plant of interest in the current study, *Erythrina caffra* (Fabaceae), is a medium-to-large sized deciduous subtropical tree native to the coastal regions of KwaZulu-Natal and the Eastern Cape provinces of South Africa [10]. In African traditional medicine the stem bark is used to treat arthritis, toothache, female infertility and infectious bacterial diseases such as tuberculosis and gonorrhoea [10-12]. Antibacterial activity has also been reported against *Staphylococcus epidermidis*, *S. aureus* and *Pseudomonas aeruginosa* [10]. In other studies, *Micrococcus luteus*, *Streptococcus faecalis*, *Serratia mercences*, *Enterococcus cloacae*, *E. faecalis*, *Proteus vulgaris*, *Shigella sonnei*, *S. flexneri*, *Escherichia coli*, *Bacillus subtilis*, *B. pumilus*, *Acinetobacter calcoaceticus anitratis*, *P. aeruginosa*, and different strains of *Klebsiella pneumonia* and *S. aureus* demonstrated susceptibility to *E. caffra* stem bark extracts [12, 13]. The antibacterial activity of the stem bark extracts has been attributed to the presence of various flavonoids, phenolics, alkaloids and tannins [10, 12, 13].

Although there are numerous reports on the efficacy of silver nanoparticles synthesised from medicinal plants against pathogenic bacteria, there are no reports on the use of *E. caffra* stem bark extracts to synthesise these nanoparticles or to test their antibacterial activity. Furthermore, in light of the increasing ability of bacteria to develop multidrug resistance against known antibiotics, there is a need to discover innovative and safe bioactive agents of plant origin. Therefore, the aims of the present study were to synthesise, characterise and quantify silver nanoparticles using aqueous stem bark extracts of *E. caffra* and to screen the synthesised nanoparticles for their antibacterial activity.

2. Experimental

2.1. Preparation of aqueous bark extracts

Fresh bark samples of *E. caffra* were collected from the University of KwaZulu-Natal, Westville Campus (29°49'04.4''S, 30°56'22.1''E) and dried at 50 °C in a laboratory oven for 48 h. Thereafter, liquid nitrogen was used to facilitate the grinding of the dried samples into fine powder using a pestle and mortar. Then, 200 ml Millipore water (Milli-Q Integral, Germany) were added to 20 g of the powder for 24 h extraction on a mechanical shaker (Labcon, South Africa) followed by vacuum filtration (Whatman no. 1 filter paper) to derive the aqueous extract.

2.2. Biosynthesis and yield of nanoparticles

Forty-five ml of 1 mM silver nitrate (AgNO_3) solution were added to 5 ml aqueous extract. The mixture was aliquoted for three incubation times i.e. 6, 12 and 24 h at ambient temperature (23 °C) and in a water bath set at 80 °C and then incubated in the light. Thereafter, the mixtures were poured into pre-weighed centrifuge tubes and centrifuged at 4 °C at 10000 rpm (Beckman Coulter, USA). The supernatant was discarded, and the remaining pellet dried at 60 °C in a laboratory oven for 48 h. The centrifuge tubes were weighed again after drying and the dry weights (nanoparticle yields) were calculated by finding the differences between the final and initial weights. The above procedure was performed three times.

2.3. Characterisation of synthesized nanoparticles

Transmission Electron Microscopy (TEM). Dried nanoparticle pellets were sonicated in ethanol using a sonication bath (Soniclean, China) and the dispersed nano-silver particles (NSPs) were separately coated onto carbon grids before being placed under a desk lamp for the evaporation of the solvent. Thereafter, the NSPs were viewed using high resolution transmission electron microscopy (HRTEM, Jeol 2100, Japan) and their shapes observed. Additionally, the TEM was equipped with energy dispersive x-ray (EDX) software (Oxford X-Max 80 mm SDD, England) which allowed for the determination of the elemental composition of the samples.

Captured TEM images were observed with iTEM Image Analysis software (v 5.0, Build 1089, Germany) to record the NSP sizes.

Fourier Transform Infra-Red (FTIR) Spectroscopy. Dried nanoparticle pellets were used to determine the functional groups capping the synthesized NSPs in a PerkinElmer FTIR Spectrum One spectrophotometer (USA) in the diffuse reflectance mode operating at a resolution of 4 cm^{-1} .

2.4. Antibacterial assays

Preparation. All culturing media and materials (e.g. glassware) were autoclaved ($121\text{ }^{\circ}\text{C}$ and 1.2 kg cm^2 for 20 min). One ml of 10% dimethyl sulfoxide (DMSO) was poured into an Eppendorf tube containing 1 mg of NSPs. The tube was then sonicated (Soniclean, China) at ambient temperature to ensure a homogenous mixture following which the mixture was diluted to $500\text{ }\mu\text{g ml}^{-1}$ with filtered DMSO. The antibiotics, vancomycin and neomycin (Sigma, South Africa) were also prepared in the same concentration as the NSPs.

Bacterial Strains. The synthesized NSPs were evaluated for their antimicrobial activity against two gram positive bacteria, viz. *Staphylococcus aureus* (ATCC 29213), methicillin-resistant *S. aureus* (MRSA, ATCC 43300) and one gram negative bacterium, *Escherichia coli* (ATCC 25922). Each species was subcultured from $-80\text{ }^{\circ}\text{C}$ bank cultures and incubated at $37\text{ }^{\circ}\text{C}$ overnight in a laboratory oven.

Agar Diffusion Assay. Working in a laminar flow, the bacterial cultures were diluted to 0.5 McFarland turbidity standards (1×10^8 Colony Forming Unit ml^{-1}) by aseptically dipping them loop by loop into 10 ml autoclaved distilled water. After each loop, the density change of the water was compared against 0.5 McFarland until the desired density was obtained. This was used as the bacterial stock for the assay. Thereafter, $100\text{ }\mu\text{l}$ of the diluted test bacterium was transferred into a Mueller-Hinton agar (MHA, Sigma®, South Africa) plate. A sterile loop was placed into the bacterial stock and streaks of the test bacterium were made on the MHA plate creating a bacterial lawn. To obtain uniform bacterial growth, the MHA plates were streaked in one direction, rotated 90° and streaked again in that direction. This rotation was done three times. A second plate was prepared in the same manner and both plates were allowed to dry for 5 minutes. A sterile cork borer was used to bore out wells ($\text{Ø } 10\text{mm}$) in each quadrant of the agar plate. In plate 1, NSPs were added into the wells in the concentrations of $500\text{ }\mu\text{g ml}^{-1}$ (filtered 10% DMSO was added to achieve the same volume per well). In plate 2, the antibiotics ($500\text{ }\mu\text{g ml}^{-1}$) were added into the wells (distilled water was added to achieve the same volume per well). Thereafter, the plates were sealed with parafilm and incubated overnight at $37\text{ }^{\circ}\text{C}$ in a laboratory oven. On the following day, the plates were examined and the zones of inhibition measured in mm using a metric ruler.

2.5. Statistical analyses

All data were analysed using the Statistical Package for the Social Sciences (SPSS) (Version 25, IBM, USA). Prior to analysis data were tested for normality using the Kolmogorov-Smirnov test ($p \leq 0.05$). Data were then analysed using a One-Way Analysis of Variance (ANOVA) and means were compared using Tukey's Post-Hoc test at the 95% confidence interval. Differences amongst treatments were represented by assigning different alphabets to the means; values that did not share an alphabet were recognised as being significantly different. Comparisons between temperatures were determined by an independent samples t-test at the 95% confidence interval.

3. Results

3.1. Biosynthesis and yield

During the incubation period, the samples changed colour from light grey to brown in the first few minutes of incubation indicating the formation of NSPs. The colour change confirmed the reduction of silver (Ag^+) to metallic silver (Ag^0) by the secondary metabolites present in the aqueous extracts. At both tested temperatures, the yield of NSPs significantly decreased after 6 h of incubation with the lowest yield ($520 \pm 7\text{ mg}$) resulting after 24 h at $80\text{ }^{\circ}\text{C}$ (Fig. 1). After 6 and 24 h

of incubation the yields were higher at ambient temperature (587 ± 2.5 and 567 ± 2.7 mg, respectively) than at $80\text{ }^{\circ}\text{C}$ (578 ± 2 and 520 ± 7 mg, respectively). For figure 1, A-C represents the statistical differences in nanoparticle yield amongst the incubation times for each tested temperature (One-way ANOVA and Tukey's Post Hoc test, mean \pm SD, $p\leq 0.05$, $n=3$); a-b represents the statistical differences in nanoparticle yield between temperatures for each incubation time (independent samples t-test, mean \pm SD, $p\leq 0.05$, $n=3$).

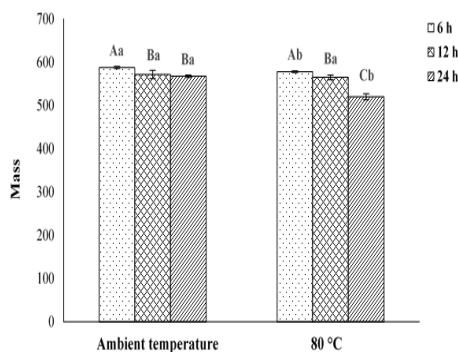


Fig. 1 The yield of nano-silver particles synthesised from aqueous extracts of *E. caffra* at different temperatures and incubation times.

3.2. TEM

NSPs were polydispersed, with some agglomeration observed, spherical in shape at both tested temperatures (Fig. 2 a, c) and their shapes were not affected by the incubation time. The EDX spectra at both tested temperatures, confirming the presence of elemental silver, are also similar (Fig. 2 b, d). The copper and carbon peaks observed in the spectra are indicative of the sample grid and support film, respectively.

The NSPs ranged in size from 2.3-29.5, 3.4-20.0 and 6.1-23.3 nm and 5.4-21.3, 5.6-16.3 and 3.7-27.4 nm at ambient temperature and at $80\text{ }^{\circ}\text{C}$, respectively (Table 1). After 24 h of incubation at ambient temperature and at $80\text{ }^{\circ}\text{C}$, the mean NSP sizes were significantly larger (14.6 ± 4.8 , 12.6 ± 5.5 nm, respectively) than those incubated for 12 (9.4 ± 4.3 , 9.7 ± 3.0 nm, respectively) h (Table 1). Amongst all the synthesised NSPs, the largest nanoparticles were obtained after 24 h of incubation at ambient temperature (14.6 ± 4.8 nm) while the smallest were formed after 12 h incubation at ambient temperature and 6 and 12 h of incubation at $80\text{ }^{\circ}\text{C}$. The majority of NSPs synthesised at ambient temperature and at $80\text{ }^{\circ}\text{C}$ were between 2 and 16 nm after 6 (77 and 90%), 12 (87 and 97%) and 24 (67 and 80%) h of incubation time, respectively (Table 1, Fig. 3 a-f).

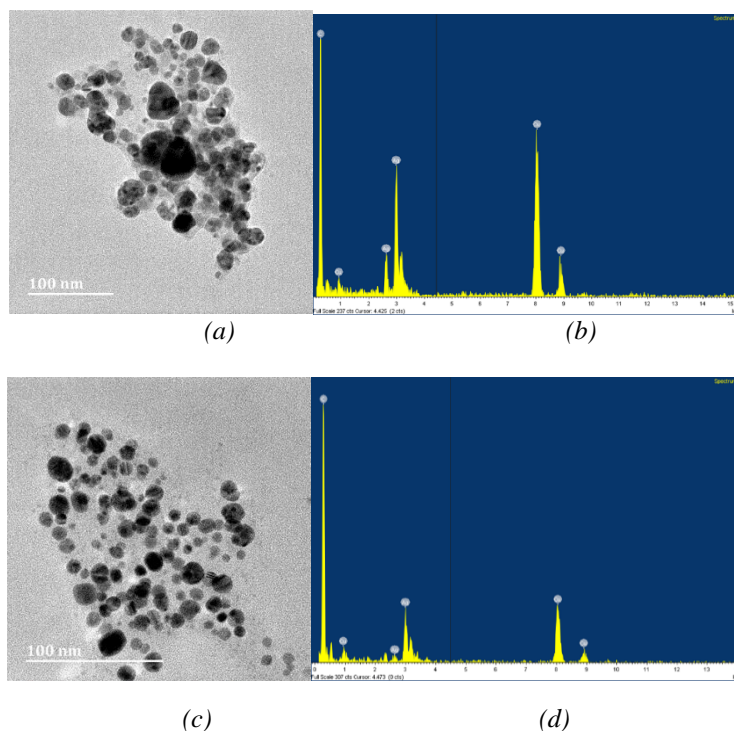


Fig. 2. HRTEM images of nano-silver particles synthesised at ambient temperature (a) and at 80 °C (c), respectively, with corresponding EDX spectra (b and d, respectively).

Table 1. Size categories, minimum, maximum and mean (\pm SD) sizes of nano-silver particles synthesized after 6, 12 and 24 h of incubation at ambient temperature and at 80 °C.

Size (nm)	Ambient temperature			80 °C		
	6 h	12 h	24 h	6 h	12 h	24 h
≤ 8	12	12	3	7	11	6
≤ 16	11	14	17	20	18	18
≤ 24	6	4	10	3	1	4
> 24	1	0	0	0	0	2
Maximum	29.5	20.0	23.3	21.3	16.3	27.4
Minimum	2.3	3.4	6.1	5.4	5.6	3.7
Mean \pm SD	11.2 \pm 7.1 ^{ABab}	9.4 \pm 4.3 ^{Bb}	14.6 \pm 4.8 ^{Aa}	10.7 \pm 3.9 ^{ABb}	9.7 \pm 3.0 ^{Bb}	12.6 \pm 5.5 ^{Aab}

Where different uppercase alphabets represent significant differences in mean sizes amongst synthesised nano-silver particles at ambient temperature and at 80 °C, different lowercase alphabets represent significant differences in mean sizes amongst all the synthesised nano-silver particles (One-way ANOVA, Tukey's Post-Hoc test, mean \pm SD, $p \leq 0.05$, $n=30$).

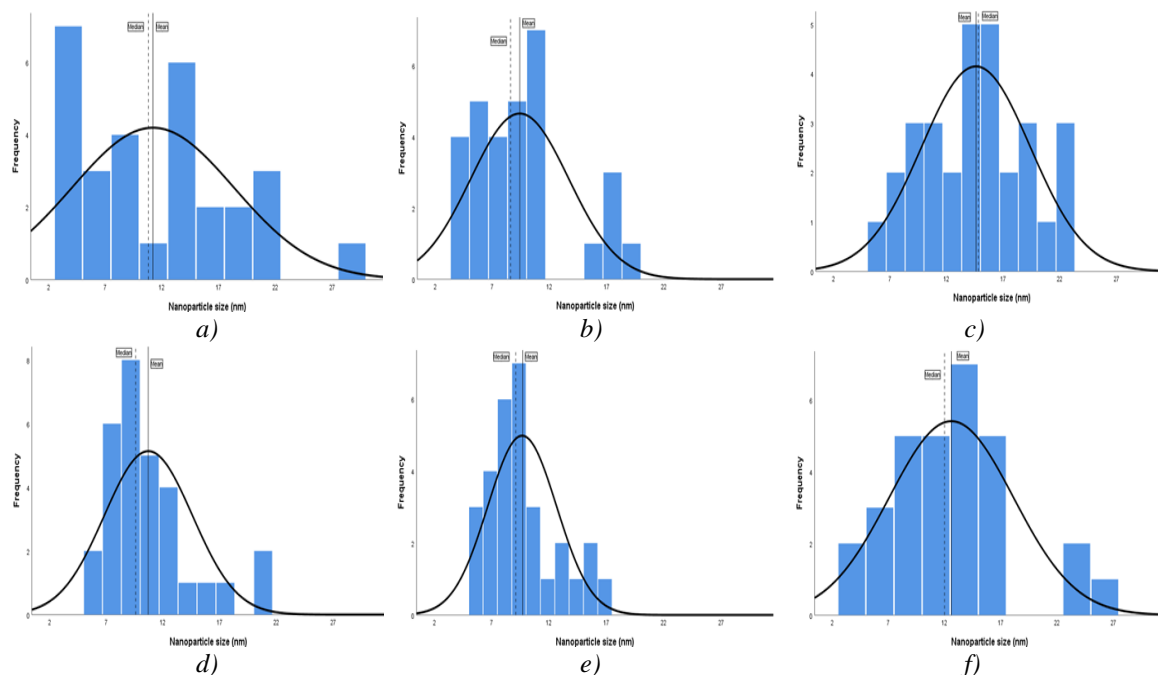


Fig. 3. Size distributions of nano-silver particles synthesised after 6, 12 and 24 h of incubation at ambient temperature (a, b and c, respectively) and at 80 °C (d, e and f, respectively).

3.3. FTIR

Fig. 4 represents the FTIR spectra showing peaks of the capping agents (functional groups) derived from organic molecules of the aqueous bark extracts associated with the synthesised NSPs. As incubation time increased, the number of peaks increased for the synthesised NSPs at ambient temperature, however, the functional groups were identical after all incubation times (Fig. 4 a). These included carboxylic acids (O-H stretching, 3223-3264 cm^{-1}), alcohols (O-H stretching, 2931-2981 cm^{-1}), alkynes (C≡C stretching, 2170-2179 cm^{-1}), amines (N-H bending and C-N stretching, 1586 and 1017-1042 cm^{-1} , respectively), phenols (O-H bending, 1319-1389 cm^{-1}), aromatic amines (C-N stretching, 1262-1280 cm^{-1}), secondary alcohols (C-O stretching, 1117-1121 cm^{-1}), alkenes (C=C bending, 616-931 cm^{-1}) and halo compounds (C-I stretching, 523-551 cm^{-1}).

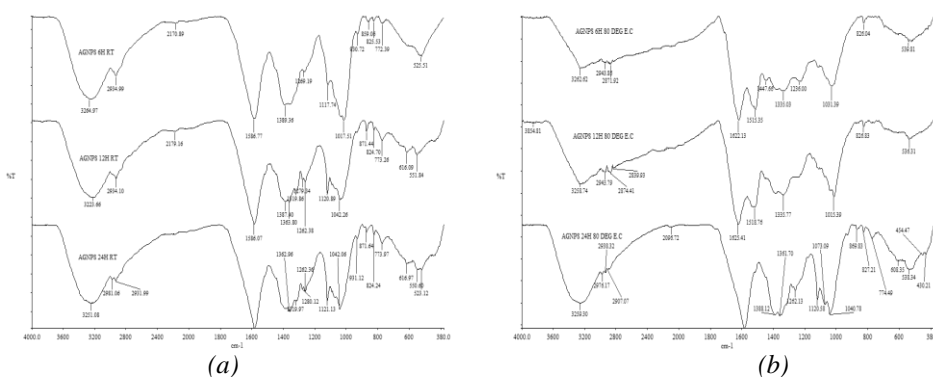


Fig. 4. FTIR spectra of nano-silver particles synthesised from aqueous extracts of *E. caffra* for 6, 12 and 24 h (top to bottom) at ambient temperature (a) and at 80 °C (b).

At 80 °C, some functional groups were common amongst the three incubation times i.e. alcohols (O-H stretching, 2871-3854 cm^{-1}), alkenes (C=C stretching and bending, 1622-1625 and 608-869 cm^{-1} , respectively), alkanes (1447 cm^{-1}), phenols (O-H bending, 1335-1388 cm^{-1}), amines (C-N stretching, 1015-1040 cm^{-1}) and halo compounds (C-I stretching, 430-539 cm^{-1}) (Fig. 4 b).

The exceptions were the presence of nitro compounds (N-O stretching, 1515-1518 cm^{-1}) after 6 and 12 h of incubation time only, and alkynes ($\text{C}\equiv\text{C}$ stretching, 2096 cm^{-1}), aromatic amines (C-N stretching, 1262 cm^{-1}) and secondary and primary alcohols (C-O stretching, 1120 and 1073 cm^{-1} , respectively) after 24 h of incubation time only.

When comparisons were made between temperatures for each incubation time, the following differences were found – after 6 and 12 h of incubation, no alkanes and nitro compounds were observed at ambient temperature and no alkynes, aromatic amines, secondary alcohols and carboxylic acids were observed at 80 °C; after 24 h of incubation, no alkanes and primary alcohols were observed at ambient temperature while no carboxylic acids were observed at 80 °C.

3.4. Agar diffusion

No antibacterial activity (observed as no zones of inhibition) was observed in the agar diffusion assay with NSPs synthesised at 80 °C. NSPs synthesised at all incubation times under ambient temperature demonstrated inhibition against all tested bacterial strains (Table 2, Fig. 5). For the tested NSPs, the zones of inhibition ranged from 14.0±1.0-16.0±0.0, 13.7±1.2-15.0±1.0 and 13.3±0.6-15.3±1.2 mm for methicillin-resistant *S. aureus*, *S. aureus* and *E. coli*, respectively, but there were no significant differences in their activity for any bacterial strain. There were no significant differences in the inhibition zones amongst the bacterial strains except for methicillin-resistant *S. aureus* which was significantly more susceptible to the NSPs incubated for 12 h than the other two strains. Similarly, both *S. aureus* strains were significantly more susceptible to vancomycin than *E. coli*, and *S. aureus* and *E. coli* were significantly more susceptible to neomycin than the methicillin-resistant strain. For both *S. aureus* strains, both antibiotics demonstrated significantly higher activity than NSPs incubated at all tested times while all the NSPs were as effective as vancomycin against *E. coli*.

Table 2. Antibacterial activity of nano-silver particles synthesised from aqueous bark extracts of *E. caffra* at ambient temperature after 6, 12 and 24 h of incubation, represented as zones of inhibition.

Time (h)/ Antibiotic	Zones of inhibition (mm)		
	<i>S. aureus</i> (MRSA)	<i>S. aureus</i>	<i>E. coli</i>
6	14.0±1.0 Ca	15.0±1.0 Ca	14.3±0.6 Ba
12	16.0±0.0 Ca	14.3±0.6 Cb	13.3±0.6 Bb
24	14.3±1.2 Ca	13.7±1.2 Ca	15.3±1.2 Ba
Vancomycin	21.7±2.5 Aa	20.7±1.5 Ba	13.7±0.6 Bb
Neomycin	18.3±2.5 Bb	25.7±2.1 Aa	24.0±2.0 Aa

Where different uppercase letters (A-C) represent statistical differences within a column and different lowercase letters (a-b) represent statistical differences across a row (One-way ANOVA, Tukey's Post-Hoc test, mean±SD, $p\leq 0.05$, $n=3$).



Fig. 5. Antibacterial activity of nano-silver particles synthesized for 12 h at ambient temperature (left) and vancomycin (right) against methicillin-resistant *S. aureus*.

4. Discussion

In metal nanoparticle synthesis, the temperature and incubation time of the reaction medium determine the nature of the nanoparticles formed [4, 14]. Most studies report on the size and morphology of the particles but there are few reports on the quantification of biosynthesised metal nanoparticles. In the present study we attempted to quantify the NSPs derived from aqueous stem bark extracts of *E. caffra* using a gravimetric approach and found that increased temperature and incubation time significantly decreased the yield of NSPs (Fig. 1). These results are contrary to those reported [15, 16] which showed that increasing incubation time (1 to 168 h and 10 to 70 min, respectively) and temperature (30 to 90 and 37 to 90 °C, respectively) increased the amount of silver nanoparticles synthesised from olive and mangosteen leaf extracts, respectively, which were determined spectrophotometrically. Similar findings to these authors were reported using different plant extracts [17]. In the latter study, it was explained that increased reaction temperature and time caused a rapid reduction and accumulation of Ag⁺ ions. In contrast, leaf extracts of *Zanthoxylum capense* produced the same quantity of synthesised silver nanoparticles at two tested temperatures (ambient and 80 °C) [18]. In the current study, both an increased temperature and extended incubation time had no further effect on the reduction of Ag⁺ ions so it is concluded that ambient temperature and 6 h of incubation time is conducive to nucleation and crystallisation in *E. caffra*-mediated NSP synthesis. This is further supported by the rapid colour change within the first few minutes when AgNO₃ was mixed with the aqueous stem bark extracts.

It is generally accepted that high temperature promotes nucleation, and low temperature is conducive to growth [19], however, the present study did not demonstrate such phenomena. Only the incubation time significantly affected the NSP size at both tested temperatures (Table 1). An increase in the size of the NSPs can be explained by the growth/agglomeration of the NSPs as the incubation time increased. In contrast, the average silver nanoparticle size decreased with an increase in temperature in a study on *Citrus sinensis* [20]. Other studies show nanoparticle size increases with an increase in temperature and/or incubation time [16, 17, 21]. Despite larger NSPs forming at an extended incubation time at both tested temperatures in the present study (Table 1), this did not translate to an increase in yield (Fig. 1) meaning that even though the particles were largest after 24 h of incubation, they were not greater in mass than those incubated for 6 h. Moreover, there was no significant difference in the antibacterial activity of the larger particles compared to the smaller ones and the incubation time also did not significantly affect the activity of the synthesised NSPs (Table 1, 2). The majority (67-90%) of synthesised NSPs derived at ambient temperature were very small (<24 nm) (Table 1) so their antibacterial activity may be attributed to this small size [9] at all incubation times (Table 2). Although the size categories of the NSPs derived from the 80 °C synthesis were similar to those at ambient temperature, no antibacterial activity was detected in the assay, and an absence of some functional groups (e.g. alkynes, aromatic amines, secondary alcohols and carboxylic acids) (Fig. 4) at the higher synthesis temperature may be attributed for this. From the FTIR spectroscopic confirmation of the functional groups capping the NSPs (Fig. 4), the presence of stem bark alkaloids and flavonoids [11, 22, respectively] can be corroborated. These compounds have been attributed for the antibacterial activity of stem bark extracts of *E. caffra* [10, 12, 13].

In the agar diffusion assay, all the synthesised NSPs demonstrated inhibition against all tested bacterial strains (Table 2) which is important because it shows their broad spectrum of activity viz. different species, gram positive/negative and methicillin-resistant. This contradicts some literature which shows that gram negative bacteria are more susceptible to NSPs compared to gram positive bacteria possibly due to the difference in the thickness and composition of their cell walls [23]. Gram positive bacteria contain a thick peptidoglycan layer containing teichoic acids which limit the uptake of silver ions while gram negative bacteria have a thin peptidoglycan layer with an outer layer of liposaccharides together with membranes containing negative electrostatic charges which attract and facilitate diffusion of NSPs [23]. It is also possible that the smallest NSPs (<24 nm, Table 1) permeated through the membrane and affected protein synthesis causing structural changes and cell death as shown in other investigations [24, 25].

The disparity between the efficacy of the NSPs and the tested standards against both *S. aureus* strains could be explained by the amalgam of the bioactive groups capping the NSPs

compared to the pure antibiotics. It is understood that vancomycin is lethal when it binds to cell wall precursors preventing gram positive bacteria from cross-linking adjacent peptidoglycan strands by peptide bonds during cell wall biosynthesis [26]. Neomycin, on the other hand, is known to be partially effective against gram positive bacteria by binding their ribosomes and inhibiting protein synthesis [27]. In the case of *E. coli*, a gram negative species, neomycin was more effective than vancomycin, as expected, however, the synthesized NSPs had similar activity to vancomycin (Table 2). This means that the NSPs in conjunction with their associated functional groups were as effective as vancomycin in inhibiting peptidoglycan synthesis thereby warranting mechanical fragility of the bacterial cell walls. Other studies have also reported on the antibacterial efficacy of green synthesized NSPs on *S. aureus* and *E. coli* [16, 20, 28, 29].

5. Conclusions

This is first report of silver nanoparticles being synthesized from the aqueous bark extracts of *E. caffra*. Synthesis temperature affected their yield and functional groups while incubation time affected their yield, size and the functional groups (at 80 °C only). All the NSPs synthesized at ambient temperature showed antibacterial activity against the three tested bacteria but they were less effective than the tested antibiotics except in the case of *E. coli*. Further work will include the synergistic effects of the biosynthesized silver nanoparticles and antibiotics on methicillin-resistant *S. aureus*, *S. aureus* and *E. coli* amongst other bacterial species.

Acknowledgements

This work was supported by the National Research Foundation (NRF) [grant numbers 81290 and the NSFAS Honours Award] and the University of KwaZulu-Natal (UKZN). The authors also acknowledge Ms. Anita Naidoo for assisting with FTIR, Ms. C. Ramlall, Mr V. Khumalo and Mr S. Maliehe for technical support and Dr J. Shaik for input on size data.

References

- [1] D. L. Feldheim, C. A. Foss (eds), Metal nanoparticles: synthesis, characterization, and applications, Marcel Dekker, Inc., New York, (2002).
- [2] A. K. Mittal, Y. Chisti, U. C. Banerjee, *Biotechnol. Adv.* **31**, 346 (2013).
- [3] S. Iravani, *Green Chem.* **13**, 2638 (2011).
- [4] M. Shah, D. Fawcett, S. Sharma, S. K. Tripathy, G. E. J. Poinern, *Materials* **8**, 7278 (2015).
- [5] V. V. Makarov, A. J. Love, O. V. Sinitsya, S. S. Makarova, I. V. Yaminsky, M. E. Tiliansky, N. O. Kalinina, *Acta Naturae* **6**, 35 (2014).
- [6] S. Ahmed, M. Ahmad, B. L. Swami, S. Ikram, *J. Adv. Res.* **7**, 17 (2016).
- [7] N. Kulkarni, U. Muddapur, *J. Nanotech.* **2014**, 1 (2014).
- [8] V. Kumar, S. Yadav, *J. Chem. Technol. Biotechnol.* **84**, 151 (2009).
- [9] A. A. Mitiku, B. Yilma, *Int. J. Pharm. Sci. Res.* **46**, 52 (2017).
- [10] J. C. Chukwujekwu, F. R. Van Heerden, J. Van Staden, *Phytother. Res.* **25**, 46 (2011).
- [11] S. El-Masry, H. M. Hammada, H. H. Zoatout, S. I. Alqasoumi, M. S. Abdel-Kader, *Nat. Prod. Sci.* **16**, 211 (2010).
- [12] O. O. Olajuyigbe, A. J. Afolayan, *Sci. World. J.* **1**, 318 (2012a).
- [13] O. O. Olajuyigbe, A. J. Afolayan, *J. Med. Plant. Res.* **6**, 1713 (2012b).
- [14] J. K. Patra, K. H. Baek, *J. Nanomater.* **2014**, 1 (2014).
- [15] M. M. H. Khalil, E. H. Ismail, K. Z. El-Baghdady, D. Mohamed, *Arab. J. Chem.* **7**, 1131 (2014).
- [16] R. Veerasamy, T. Z. Xin, S. Gunasagan, T. F. W. Xiang, E. F. C. Yang, N. Jeyakumar, S. A. Dhanaraj, *J. Saudi. Chem. Soc.* **15**, 113 (2010)

- [17] J. Y. Song, B. S. Kim, *Bioprocess. Biosyst. Eng.* **32**, 79 (2009).
- [18] O. Bodede, S. Shaik, R. Govinden, R. Moodley, *Adv. Nat. Sci-Nanosci.* **8**, 1 (2017).
- [19] H. Liu, H. Zhang, J. Wang, J. Wei, *Arab. J. Chem. In Press* (2017).
- [20] S. Kaviya, J. Santhanalakshmi, B. Viswanathan, J. Muthumary, K. Srinivasan, *Spectrochim. Acta. A. Mol. Biomol. Spectrosc.* **79**, 594 (2011).
- [21] S. Li, Y. Shen, A. Xie, X. Yu, L. Qiu, L. Zhang, Q. Zhang, *Green Chem.* **9**, 852 (2007).
- [22] Z. Y. Desta, N. Sewald, R. R. T. Majinda, *Nat. Prod. Res.* **28**, 667 (2014).
- [23] E. Pazos-Ortiz, J. H. Roque-Ruiz, E. A. Hinojos-Márquez, J. López-Esparza, A. Donohué-Cornejo, J. C. Cuevas-González, L. F. Espinosa-Cristóbal, S. Y. Reyes-López, *J. Nanomater.* **2017**, 1 (2017).
- [24] I. Sondi, B. Salopek-Sondi, *J. Colloid Interface Sci.* **275**, 177 (2004).
- [25] C. S. Ciobanu, S. L. Iconaru, M. C. Chifiriuc, A. Costescu, P. le Coustumer, D. Predoi, *BioMed. Res. Int.* **2013**, 1 (2013).
- [26] P. Courvalin, *Clin. Infect. Dis.* **42**, S25 (2006).
- [27] M. Y. Fosso, Y. Li, S. Garneau-Tsodikova, *MedChemComm.* **5**, 1075 (2014).
- [28] R. M. Ali, L. Umaralikhan, M. J. M. Jaffar, *Int. J. Appl. Biol. Pharm.* **6**, 115 (2015).
- [29] T. Dhanalakshmi, S. Rajendran, *Arch. Appl. Sci. Res.* **4**, 1289 (2011).